

NASA TECHNICAL MEMORANDUM

NASA TM-77785

PROFILE DESIGN FOR WINGS AND PROPELLERS

A. Quast and K.H. Horstmann

NOT TO BE TAKEN FROM THIS BOOK

Translation of "Profilauslegung fuer Tragfluegel und Propeller,
IN: Problems and Development Trends in General Aviation; Symposium,
Friedrichshafen, West Germany, March 24-25, 1983; Bonn, Deutsche
Gesellschaft fuer Luft- und Raumfahrt, 1983, pp. 107-138

1983 3 29

LANGLEY RESEARCH CENTER
LIBRARY, NASA
HAMPTON, VIRGINIA

STANDARD TITLE PAGE

1. Report No. NASA TM-77785	2. Government Accession No.	3. Recipient's Catalog No.	
4. Title and Subtitle Profile Design for Wings and Propellers		5. Report Date December 1984	
		6. Performing Organization Code	
7. Author(s) A. Quast and K.H. Horstmann		8. Performing Organization Report No.	
		10. Work Unit No.	
9. Performing Organization Name and Address Leo Kanner Associates P.O. Box 5187 Redwood City, CA 94063.		11. Contract or Grant No. NASW-4005	
		13. Type of Report and Period Covered Translation	
12. Sponsoring Agency Name and Address National Aeronautics and Space Administration Washington, D.C. 20546		14. Sponsoring Agency Code	
		15. Supplementary Notes Translation of "Profilauslegung fuer Tragfluegel und Propeller, IN: Problems and Development Trends in General Aviation; Symposium, Friedrichshafen, West Germany, March 24-25, 1983; Bonn, Deutsche Gesellschaft fuer Luft- und Raumfahrt, 1983, pp. 107-138. (A84-15411)	
16. Abstract <p>It has now become customary to develop profiles for wings and propellers for a given employment of the aircraft. This is possible because methods and computers are available to study an entire series of variants in a comparatively short time. The basic viewpoints for profile design are presented. It is shown that laminarizaion has its advantages in almost all cases, including the design of a turbine blade and the design of the profile of an airliner. The requirements which profiles have to satisfy are discussed along with the possibilities for increasing lift on profiles. Attention is given to friction-related drag, and drag related to pressure conditions. The effect of fouling on laminar profiles is also considered.</p>			
17. Key Words (Selected by Author(s))		18. Distribution Statement Unclassified - Unlimited	
19. Security Classif. (of this report) Unclassified	20. Security Classif. (of this page) Unclassified	21. No. of Pages 31	22.

PROFILE DESIGN FOR WINGS AND PROPELLERS

A. Quast and K.H. Horstmann

i	Contents Notations:	
1.	Introduction	1
2.	Requirements for the profile	1
3.	Possibilities of increasing the lift on profile	2a
	3.1 Individual profiles	2a
	3.2 High lift aids	3
4.	Resistance mechanisms	4
	4.1 Friction resistance	4
	4.2 Pressure resistance	6
5.	Layout of profiles	8
6.	Effect of contamination on laminar profile	11
7.	Summary	13
8.	Literature	13
	Tables	15
	Figures	17

Notations

c_A		Lift coefficient of the aircraft
c_a		Lift of the profile
$c_{a \max}$		Maximum lift coefficient
c'_f		Coefficient of local resistance
c_w		Resistance coefficient of the aircraft
c_{w0}		Coefficient of noninduced resistance
c_{wi}		Coefficient of induced resistance
c_{ws}		Coefficient of harmful resistance
c_{wp}		Profile resistance coefficient
c_p		Pressure coefficient
d	[m]	Profile thickness
E		Lift-drag ratio
l	[m]	Profile depth
Ma		Mach number
Re		Reynolds number
Re_x		Reynolds number formed with the run length
x	[m]	Coordinate in the direction of the profile chord
α	[degree]	Angle of incidence
δ_1	[m]	Displacement thickness of the boundary layer
δ_2	[m]	Pulse loss thickness of the boundary layer
η	[degrees]	Flap angle
Λ_{eff}		Effective (aerodynamic) extension

1. Introduction

Whereas earlier profiles for wings and propellers were sought from profile catalogues, now-a-days they have started developing to an increasing extent profiles for a certain purpose. This has become possible, because meanwhile methods and computers are available making it possible to study a large number of variants within a relatively short time.

The basic aspects of profile design are described below. It is shown, that the laminarization is almost always advantageous, from the turbine blade until the profile of the commercial aircraft. Moreover layout limits such as turbulent detachment, Ma-number and contamination by insects are discussed.

2. Requirements for Profile

The purpose of a profile is basically to produce a lift, a specifically with the minimum possible resistance. The resistance on the wings consist in the first approximation of noninduced and induced resistance.

$$c_W = c_{W0} + c_{Wi}$$

The component of the induced resistance is

$$c_{Wi} = \frac{c_A^2}{\Lambda_{\text{eff}}}$$

where c_A is the lift coefficient and Λ_{eff} is the effective extension which gives approximately the ratio of the span to the average wing depth. In turbine machines, the edge and slit losses can also be considered as induced resistance.

To be able to operate in a prop with the minimum possible energy requirement, it is necessary, that the ratio of the lift c_A to the resistance c_W be the maximum possible at the layout point. This ratio c_A/c_W , also called lift-drag ratio E , is large, if either c_A is large

*Numbers in margin indicate pagination in foreign texts.

and c_W is small.

$$E = \frac{c_A}{c_W} = \frac{c_A}{c_{Wi} + c_{Wo}}, \quad c_{Wo} = c_{wp} + c_{Ws}$$

/110

c_{Wo} : noninduced resistance

c_{Ws} : harmful resistance (Fuselage, empennage or gondola resistance)

c_{wp} : Profile resistance

The lift-drag ratio of aircraft corresponds in propellers and turbine machines to the efficiency.

Figure 1 shows the variation of the lift-drag ratio against the lift coefficient for a commercial aircraft. The left part of the Figure shows the variation of the effective extension, the right hand portion the profile resistance. Modern commercial aircraft have extensions up to $\Lambda_{eff} \approx 9$ (A310) and a profile resistance of $c_{wp} \approx 0.006$. With the increasing energy costs, future commercial aircraft will probably have higher wing extensions $\Lambda_{eff} \approx 10 \dots 12$ and a profile resistance which will for laminar profile be at c_{wp} 0.003. Figure 1 shows a very flat optimum for the lift-drag ratio, while the c_A value of the optimum is a function of extension and resistance. The optimum lift-drag ratio, for which c_A/c_W is a maximum is reached, when the induced resistance is equal to the noninduced resistance:

$$c_{Wi} = c_{Wo}$$

This means, that induced and noninduced resistances are equally important in aerodynamic studies. Similar remarks also apply to propellers and turbine machines. Because of the low effect extension of propellers, here the lift coefficient has optimum efficiencies for $c_A \approx 0.3$

The next sections will discuss how on one hand the lift coefficient c_A can be increased or how it is possible to maintain the resistance coefficient c_W small, to achieved to maximum values of the lift-drag coefficient.

3. Possibilities of Increasing the Lift on Profiles

/111

3.1 Individual Profiles

The lift of a profile is obtained from the integration of the difference in pressure between the top and bottom of the profile. This difference of pressure can be increased by the camber and the angle of incidence.

In the previous chapter we saw, that for optimum lift-drag coefficient, maximum lift coefficient up to $c_A \approx 0.9$ are needed. This lift coefficient is achievable with almost every profile for low mach numbers of the incident flow. For higher incident flow mach numbers, however, supersonic flow occurs however on the top side of the profile, which can be delayed often only by a compression impact to supersonic velocity. The compression impact run anisentropically and can cause considerable additional resistance. But with suitable shaping of the profile local mach numbers up to mach ≤ 1.3 are achievable, without the occurrence of considerable additional resistance. With this boundary condition we obtain a minimum under pressure for the topside of the profile, below which one should not go, and which leads thus to a limitation of the lift depending on the mach number.

Therefore an attempt must be made to obtain a lift wherever this does not lead to too great an increase in lift resistance. A very trivial method is to reduce the profile thickness, with simultaneous increase of the camber, so that the top contour is maintained. Then higher pressure on the bottom of the profile, with equal pressure on the top, leads to more lift. But since thin wings become heavier, only a limited gain can be obtained. But on the bottom before and after the spar region, somewhat more lift can be obtained, since here the contour is included on the bottom. This is called "front" and "rear-loading". Both effects are shown schematically in Fig 2b,c. With both measures lift can be obtained only to a limited extent, since behind the "front-loading" range and therefore "rear-loading" range, we find increased velocities of flow and therefore losses of lift, as are shown in Fig 2b,c.

As already mentioned, on the profile top, the fact that local supersonic velocities are quite permissible may be used when the local mach number does not exceed certain values.

/112

The gain in lift through a supersonic field is then maximum, when

the local mach number has the maximum value in the region of the profile tip (Ma 1.3), then an approximately linear isentropic increase in pressure occurs, so that at about 60-70 % of the wing depth, only a weak compression impact hardly effective against resistance can occur, which lead once again to subsonic velocity. This so-called "slopy" pressure distribution is shown in Fig 2a. Here therefore some propulsion can still be obtained in the region of the profile tip.

This form of pressure distribution in the region of the supersonic field is achieved, while near the profile tip, high supersonic velocities up to $Ma \approx 1.3$ are produced by a contour element with relatively strong curvature. Immediately thereafter, the contour must run very flat, to limit a further expansion of the supersonic field and to achieve once an isentropic recompression. But the contour curvature must also not be too small, since otherwise a compression shock can occur relatively forward on the profile. Figure 3 shows the contour and the supersonic fields of such a modern transsonic profile as compared with an ordinary profile.

3.2 High Lift Aids

For high lift aids, the superficial enlargement is used primarily. For modern high lift devices with flat and a fowler flap, it is about 30% and increases the lift coefficient by 3.5 (referred to the actual wing depth) to nominally 4.5 (referred to the retracted wing depth). The increase in camber leads to a limited extent also to higher lift. Here with suitable shaping lift coefficients of 2 to 2.5 may be achieved, but without slits and referred to the actual wing depth.

The lift coefficient of 3.5 already indicated above, referred to /113 the actual wing depth is achieved only when energy is added to the boundary layer in between. This takes place through slits, so that each wing unit (slat, main wing, flap) the boundary layer begins practically anew. The slit width is obtained from the condition that the wake of a wing portion lie precisely outside the boundary layer of the next portion of the wing. The effect of this type of energy supply is shown in Fig 4. It shows the measured pressure distribution of the DFVLR (Federal German Aeronautics and Space Research Organization) high lift system Q/R4 shortly before reaching the maximum lift coefficient

for a Reynolds number $R_3 = 1.5 \times 10^6$. The dashed line shows a pressure variation assumed to be free from friction, which would be adjusted with closed slits. But on such a profile the flow would be detached already far forward, because it would have to be delayed between the tip and the rear edge by about a factor of 4 in the velocity. In this form of pressure distribution, however, it undergoes a delay of only a factor of 2. With higher Reynolds numbers, the permissible delay becomes larger. For open slits, the velocity ratio between the tip and the rear edge of each wing element is about 2. This means that the boundary layer of each individual element is stressed to the extreme. This occurs through a suitable combination of angles of incidence, angles of the slats and the fowler flap (the tip of the slat is fixed to the basic profile), in such a way that in the area of the profile tip the minimum possible excess velocities occur. This can be calculated by means of suitable computer programs.

Altogether it should be possible to achieve the present maximum lift coefficient of 4.5 even without slats, if instead of the fowler flap of Fig 4, a well-laidout double slit flap is provided. This would represent less construction cost, weight and resistance. Besides this the omission of the slat is indeed the condition for the use of laminar profiles.

4. Resistance Mechanisms

4.1 Friction Resistance

The friction resistance is obtained by integration of the wall shear stresses on a profile. /114

Figure 5 shows schematically the variation of the displacement thickness δ_1/l , the pulse loss thickness δ_2/l and the local friction resistance c'_f over the run length x/l on a flat plate. A second scale shows the run lengths-Re number Re_x . In the left part of the Figure it is assumed that the laminar-turbulent reversal takes place at $Re_x = 3 \cdot 10^6$. This corresponds approximately to the conditions in a laminar wind tunnel. In free flight we would have to take our $Re_x = 7 \cdot 10^6$ *. In the right hand portion of the image it is assumed, that the laminar-turbulent reversal takes place through a turbulator at $Re_x = 1 \cdot 10^6$. The displacement thickness δ_1 increases in the region

*Verbal information from W. Pfenniger.

of the laminar flow first as $\delta_1 \sim x^{1/2}$. The reversal is characterized by a decrease of the displacement thickness to about half. This "corner" may be seen even in profile pressure distribution for not too high Reynolds numbers. The displacement thickness of the turbulent boundary layer increases clearly more than for laminar boundary layer and specifically as $\delta_1 \sim x^{4/5}$. For the pulse loss thickness δ_2 the conditions are similar to those of the displacement thickness, only naturally no decrease of the pulse loss thickness occurs through laminar turbulent reversal.

The local resistance coefficient c'_f is very high first on the front edge, then decreases very strongly and reaches very low values. The beginning of the turbulent flow is characterized by very high wall shear stresses, which indeed become smaller quickly but in the final run also remain at a very high level as compared with that of the laminar flow.

The maximum turbulent wall shear stresses are higher by about 25% if the laminar starting section of $Re_x = 3 \cdot 10^6$ is reduced to $1 \cdot 10^6$. Further behind the reversal point, this effect decreases.

The average of the local resistance coefficient c'_f if the plate /115 resistance c_w . It may be seen from Figure 5, that the plate resistance for long laminar run length amounts to only 60% of the resistance for short laminar run length. This is also clear in the final value of the pulse loss thickness.

A more thorough consideration shows, that the resistance can already be reduced considerably, if only relatively short laminar starting distances are provided. For example for a profile unequal run length must be of 60%, even run lengths of only 20-30% reduce the resistance to a very considerable extent. To achieve this, the profile tip must be kept free from rivets, rubber, deicing units etc.

Nothing changes in the basic variation of the displacement and pulse loss thickness δ_1 and δ_2 as well as the local resistance coefficient c'_f over the run length, when accelerated (decrease in pressure) or delayed flow (increase in pressure) occurs. The numerical values vary naturally, and specifically in such a way, that for accelerated flow δ_1 and δ_2^* are smaller than for unaccelerated flow, but the

*Accelerated or delayed flow δ_2 is nonidentical to the pulse loss (resistance) comes, since δ_2 does not take into consideration the local velocity.

wall shear stress becomes larger. For delay flow, δ_1 and δ_2^* become larger, on the other hand c'_f smaller. The decrease of c'_f for delayed flow does not mean now that profiles with strongly delayed flow have a lower resistance. Unfortunately the increase of the displacement thickness caused by the reduction of c'_f causes additional pressure resistance, which will be discussed further below and what is much more important, delayed flows tend considerably to detachments of the boundary layer.

For accelerated flow, because of the increased walled shear stress as compared with accelerated flow, one should always note the laminar flow. This applies particularly to profile and fuselage tips.

4.2 Pressure Resistance

Physically it is not absolutely correct to differentiate between /116 friction and pressure resistance. But it is easier to understand if both resistance mechanisms are considered separately. By pressure resistance we understand hereafter the additional resistance, which is caused by the effect of displacement of the boundary layer and detachments* and by compression impacts. The pressure resistance is obtained by integration of the distribution, where only the component in the direction of flow is taken into consideration.

Hereafter the effect of the displacement effect of the boundary layer, the detachment of the rear edge, the laminar detachment bubbles and the compression impact on the pressure resistance will be discussed.

For a friction free flow (potential flow) the suction and pressure forces effective in front of the maximum thickness are exactly equal to the forces applied behind the thickness maximum. The force acting in the direction of flow is accordingly 0 (d'Alembert Paradox).

In the flow affected by friction, there always remains a force acting in the direction of flow, the so-called pressure resistance. This is due to the fact that the pressure distribution is altered by boundary layer displacement, detachment and impacts in the manner shown in Fig 6a.

The alteration of the pressure distribution through the boundary layer displacement is caused mainly by the delayed turbulent boundary

*Laminar and turbulent detachment bubbles, rear edge detachments.

layer in the increase of pressure, whose displacement thickness increases very strongly. As already mentioned, the pressure resistance occurring causes mostly a compensation or even over-compensation of the reduced friction resistance. The detached flow may be considered as a particularly strong thickening of the boundary layer, since here the boundary layer is detached from the surface and back flow occurs. In detachments of the rear edge, a clear decrease takes place in the rear edge pressure (Fig 6b). Increased resistance as a result of the detachment is generally observed, when the pressure coefficient on the rear edge c_{pHK} begins to become negative. A region of constant pressure in front of the rear edge indicates a very strong detachment. /117

Laminar detachment bubbles arise through laminar detachment, subsequent laminar-turbulent reversal and turbulent reapplication. The bubble represents a thickening of the contour. This changes the pressure distribution in the manner indicated in Fig 6c. Within the bubble eddies occur. In the front part of the bubble there is both a weakly rotating laminar eddy, in the rear portion a strongly rotating turbulent eddy. Large laminar detachment bubbles increase the resistance whereas small flat bubbles are not noticeable in the resistance. Laminar detachment bubbles occur in particular in model flight profile and flow machine (Re number 100,000 to 300,000). In glider aircraft, detachment bubbles also cause increased resistance in the region $Re \approx 1.5 \cdot 10^6$ and must be eliminated with turbulators or by controlled instabilization of the boundary layer. For higher Re numbers Re more than $3 \cdot 10^6$, they hardly act any longer on the resistance, since the size of the bubble decreases among other things with increasing Re number.

There are also turbulent detachment bubbles with turbulent detachment and turbulent reapplication, for example in large trailing edge flap angles on the contour bend between profile and flap.

The acceleration of the flow to the supersonic range does not pose any problems. In the deceleration from supersonic to subsonic ranges, on the other hand compression shocks almost always occur. In these compression shocks, the flow is decelerated from supersonic to subsonic range on fraction of millimeters in the direction of flow. Here a lot of energy is lost by throttling (impact losses), which would not have been lost with the continuous deceleration. The pressure

varies as discontinuously as the velocity. This is shown in Fig 6d*. The energy lost in the compression shock is noticeable on the profile as resistance. This resistance is called, not quite relevantly "wave resistance." By suitable shaping of the profile surface, as indicated in Chapter 3.1, it is possible to achieve for a narrow range of mach numbers and angles of incidence an almost impact free flow deceleration (impact free recompression of the isentropic recompression).

For practical profiles, a small impact may be permitted in most cases, which make the lift higher. But the increase of resistance is still small.

5. Layout of the Profile

With regard to a small profile resistance laminar flow should be provided wherever there are no other objections against it. The increase of pressure in front of the rear edge should be precisely such that for profile with turbulent flow around it (fouled profile tip), the flow begins to be detached on the rear edge. The rear portion of the profile should be as thin as possible, this will keep the rear edge pressure low and the flow must be decelerated to some extent. This again may be used for longer laminar run lengths on the top.

It is apparent from what was stated above, that from the known or assumed boundary layer qualities, desirable pressure distributions may be developed. Naturally a profile cannot be obtained for each pressure distribution. Moreover most profiles are designed on several design purposes. Profiles for commercial aircraft have only one design goal, specifically cruising flight, glider aircraft and propellers have three, and helicopters even more, [1], [2].

Hereafter we will discuss briefly the layout of transsonic profiles, laminar profiles for high velocities, glider aircraft profiles and propeller profiles.

Figure 7 shows the pressure distribution of a transsonic profile, as corresponds to the state of the art. In the region of pressure distribution above c_p^* , supersonic velocity occurs locally on the profile. The supersonic field is rather large and gives a considerable portion of the lift. The maximum excess velocity (mini-

*The same profile cannot have alternately an impact free and impact and impact stressed recompression. The effects shows occurs for a mach number variation of 0.75 and 0.77.

mum pressure) is to be found on the profile tip, then follows a slow deceleration, with which it should be possible primarily to avoid compression impass. The transition to the subsonic range for $x/l = 0.65$ can take place impact free or through a weak impact. Then follows the normal subsonic increase of pressure for the rear edge. The bottom shows a strong "rear-loading." The arrow indicates the presumable laminar-turbulent reversal. Through the reversal point which lies far forward on the top, the resistance is very high because of the long turbulent boundary layer with $c_{wp} = 0.006$. With such pressure distributions naturally relatively high lift coefficients can be achieved for high mach numbers. /119

On the other hand the pressure distribution of the laminar profile for commercial aircraft should appear as shown in Fig 8. Because of the long acceleration section on the top and bottom, the reversal point lies at about 50% of the profile depth. The profile resistance to be expected depends to some extent on the Re number, and according to theoretical calculations is $c_{wp} = 0.003$ for $Re = 30 \cdot 10^6$. Such resistances are in no way unrealistic and have already been measured in NACA profiles. Only the laminar profile shown is thinner than the transsonic profile shown in Fig 7, so that the comparisons of the profile from Fig 7 cannot be carried out. For the same thickness the mach number would have to be reduced, because a recompression to a great extent free from impact can only take place over a relatively long run length, as is given in Fig 7.

Laminar profiles for high Re numbers have a very sharp tip, because for high Re numbers accelerated flow is required, to secure laminar flow. The lower the Re number, the rounder the profile tip.

Basically the transsonic requirements, which lead because of the maximum possible lift to the minimum of pressure at the profile tip, and the requirements for laminarization, which require a minimum of pressure at 50 to 70% of the profile depth are basically contradictory.

Commercial aircraft with laminar profiles will therefore fly more slowly than modern commercial aircraft, but have a better lift/drag ratio [3]. With regard to the economy, these two effects are opposite. Increasing fuel costs tend to favor the laminar profile.

But it is sure, that for all aircraft flying under $Ma = 0.65$, laminarization is convenient. Such a profile is shown by Fig 9 together /120

with the calculated pressure distribution. It could be applied between Re numbers of $10 \cdot 10^6 - 30 \cdot 10^6$. The profile resistance is at approximately $c_{wp} = 0.003$.

The measurement of such laminar profiles raises considerable problems, since obviously even for laminar channels turbulence and noise affect the laminar-turbulent reversal and therefore the resistance. For high Re numbers, therefore in the wind tunnel, higher resistances may be expected than in free flight. Because of the absence of suitable experimental institutions, for example the methods to calculate the accelerated laminar boundary layer is still affected by certain factors of uncertainty.

The laminar boundary layer is stabilized by high mach numbers. Here therefore no problems need be expected, only possibly for want of suitable experimental institutions (transsonic wind tunnel for Re numbers with low noise and turbulence level) the effect cannot be used fully.

Figure 10 shows the pressure distribution and polar curve of the plane flap profile HQ 17, which incorporated in the glider aircraft ASW-22. Laminar detachment bubbles arise because of the low Re number. Basically detachment bubbles may be avoided indeed through an instablization section according to Wortmann*, but only for a certain Re number, an angle of incidence and flap angle. In particular on the bottom of the profile, laminar detachment bubbles cannot be avoided, but they may be reduced by instabilization sections. In the present case, the detachment bubbles were eliminated by blowing turbulators. Thus it is possible to reduce noticeably the resistance. Blowing turbulators are small holes (0.6mm diameter \emptyset), from which of the laminar detachment points, small amounts of ram air is blown out. Thus the flow becomes turbulent and the detachment bubble disappears entirely or partly. The profile HQ 17 has for $Re = 3 \cdot 10^6$ and blowing turbulators a minimum resistance of $c_{wp} = 0.004$, which may be seen from Fig 10 [4].

Figure 11 shows polar curves and pressure distributions of the propeller profile DFVLR-P2 as compared with a Hartzell propeller profile. It may be recognized that the P2 is better in all areas, in particular the maximum lift coefficient at the take-off ($Ma = 0.55$)

/121

*The range of weakly decelerated laminar flow in front of the intense deceleration (increase of pressure) with turbulent flow.

is higher and in cruising flight ($Ma = 0.65$) the resistance is lower. The c_a region for take-off at cruising flight is recorded in both polar diagrams. The pressure distributions of both profiles show, that the Hartzell profile has strong pressure peaks at the tip. On the other hand the profile P2 has at $c_a = 0.5$ constant pressure on the suction side. For the existing Re number of $2.5 \cdot 10^6$, laminar flow may be expected up to $x/l = 0.7$. The bottom could be laminar up to about 40%*. For higher c_a values, the top would be increasingly turbulent, while the bottom becomes increasingly laminar. This means that either the top is laminar or the bottom. For the pre-assigned thickness on the desired high maximum lift coefficient, it is not possible to maintain both top and bottom laminar simultaneously. For a thicker profile, large supersonic fields therefore effective with regard to resistance would occur. The filled measurement points in Fig 11 show the presence of supersonic fields on the bottom or top of the profile. It may be seen, that the presence of a supersonic field need not lead at all to an increase in the resistance.

6. Effect of Fouling on Laminar Profiles

In Fig 12 the polar curves of the NAS laminar profile NLF (1)0416 and the known NACA 23015 are compared [5],[6]. In the upper portion of the figure, the polar curves are shown for smooth surface and in the lower portion with artificial transition or standard roughness.

It may be recognized that the laminar profile in particular for the best lift/drag coefficient (about 0.7) has a clearly lower resistance than the NACA 23015 profile. The maximum lift coefficient is also even somewhat higher.

In artificial transition the resistance is higher as expected, /122 the $c_{a \max}$ remains however totally uninfluenced by it. The increase of resistance in artificial transition is not particularly large, it is less than for NACA 23015, while for the latter standard roughness was used. The comparison is not correct to that extent. With the artificial transition the fouling of the profile tip by striking insects should be simulated. According to the measurements of Boermans and

*The measurements were carried out in the Transsonic Wind Tunnel in Braunschweig, whose noise level is very high just like in all transsonic tunnels. The measured resistances might therefore be higher than those occurring in reality.

Selen [7], with the artificial transition, higher resistances are produced than with the real fouling by insects. It was also impossible for the case of the glider aircraft profile HQ 17 shown in Figure 7 to establish any decrease of $c_{a \max}$ when the top flow was rendered turbulent artificially by rhombus shaped turbulators in 5% of the wing depth.

Accordingly it is possible to design laminar profiles whose $c_{a \max}$ and $c_{a \max}$ variation is independent of whether the tip of the wing is clean or fouled. The laminar profile thus does not represent any safety risk. Suitable measurements are lacking, but the comparison in Fig 12 permits us to draw the conclusion, that laminar profiles, which tolerate a fouled profile tip, have in the fouled state the same or lower resistance than the likewise fouled conventional profiles. In the clean state, laminar profile are however, clearly superior in resistance. Since most of the year is "free from insects", the use of laminar profiles is reasonable even under practical conditions, because most of the time it is possible to fly with low fuel consumption as compared with previous aircraft. Moreover there are possibilities of preventing the effect of insects, by pressing out liquid for example from microscopically small holes in the region of the profile tip (NASA System). No insects can then adhere to the liquid film formed. This system requires to be connected only for air "containing insects", for example at the time of take-off and landing. This system may also be used possibly for de-icing.

According to the experience with flight measurements, the critical roughness height for laminar flow seems to be clearly larger in free flight than in the wind tunnel. This applies also to laminar wind tunnels. Probably turbulence and noise of the tunnel becomes greater with contour disturbances. In any case, the slight fouling, which lead in the wind tunnel to laminar turbulent reversal, do not lead in any way to this reversal in free flight. Therefore with regard to the fouling of laminar profiles, there is more clearance than previously imagined. The problems with suitable or tolerable experimental units remain however. In the final analysis it will be necessary to resort to flight experiments to an increasing extent. /123

7. Summary

For a good lift/drag number for aircraft and a good efficiency for propellers, rotors and flow machines, small profile resistances are important, because for the best lift/drag coefficient and optimum efficiency, the induced and noninduced resistances are precisely equally large. The noninduced resistance proves the profile resistance, besides the fuselage and empennage resistance.

An optimum lift/drag ratio requires in aircraft a lift coefficient of about 0.7, propellers of optimum efficiency require a lift coefficient of 0.3.

These lift coefficients can generally be achieved without difficulty, if the mach number is less than 0.6. In particular for wing profile we find that starting from this mach number, difficulties arise with local supersonic fields, which require compromises.

It is found that laminar flow, even if it is over only a short starting distance, always reduces the resistance. On the basis of profiles for commercial aircraft, commuter aircraft, glider aircraft and propellers, the extent to which laminarization may lead to reductions in resistance is shown.

Measurements have shown that suitably laid-out laminar profiles do not give any reduced maximum lift in case of fouling. The resistance coefficient for fouled profile is not higher or hardly higher than the fouled conventional profile.

The fact that in the wind tunnel the slightest surface disturbances lead to the laminar-turbulent reversal, whereas it is not the case in free-flight, is unfavorable for the development of aircraft. This is related to the residual turbulence and noise in the wind tunnel.

With the computation methods known today, it is possible to design profiles for various purposes, in particular knowledge is required on laminar-turbulent reversal and turbulent detachment. A design requires now as much as ever much testing, in particular if several design aspects must be considered.

8. Literature

[1] Horstmann, K.H.
Koster, H.
Quast, A.

Development of Four Profiles for an
Experimental Propeller in the Power
Class 750 Hp.

Annual Conference of the DGLR, Stuttgart
October 5-7, 1982

- [2] Horstmann, K.H.
Koster, H.
Polz, G. Development of New Airfoil Sections for Helicopter Rotor Blades.
8th European Rotorcraft Forum Aix-en-Provence, August 31-September 3, 1982.
- [3] Quast, A. Laminar Profiles for Commercial Aircraft
DFVLR Mitt. 80-07, Loh 1980.
- [4] Horstmann, K.H.
Quast, A. Decrease of Resistance Through Blowing Turbulators
DFVLR FB 81-33, Koln, 1981
- [5] Sommers, D.M. Design and Experimental Results for a Natural Laminar Flow Airfoil for General Aviation Applications.
NASA Technical Paper 1861, June, 1981. Hampton, Virginia.
- [6] Abbott, I.H. Theory of Wing Sections.
Dover Publications Inc., New York, 1959.
- [7] Boemans, L.M.M.
Selen, H.J.W. On the Design of Some Airfoils for Sailplane Application.
Report LR 326 Delft University of Technology, Delft/Niederlande. April, 1981. XVII Ortiv Kongress, Paderborn.

TABLE I

Model	Type of aircraft	Drive	Number of Passengers	Cruising altitude km	Cruising velocity km/h	Cruising Ma number	Mass load m/f	Wing Area m ²	Extension	Span m	wing depth Internal/External	Cruising RE number Wing 10 ⁶ internal/external	Fuselage m	Cruising Re number fuselage · 10 ⁶
ASW-10	SF	-	(1)	1	140	0.11	32	11	20	15	0.9/0.4	2/1	6.8	17
Robin DR 400	M	1P	4	3.5	290	0.21	70	13.6	5.6	8.7	1.7/0.9	6/3	7	25
Cesana 310	M	2P	6	3	270	0.22	190	16.6	7.3	11.3	1.7/1.2	7/5	9.7	30
Beech King Air 90	G	2P	10	6.4	400	0.35	180	27.3	8.5	15.3	2.2/1.1	10/5	12.2	94
Gates Lear Jet 24	G	2S	6	13.7	770	0.75	270	23.3	5.0	10.8	2.7/1.4	10/5	12.5	45
Fekker F27	V	2P	34	6.1	480	0.42	290	70	12	29	3.5/1.4	19/8	25	137
Fekker F28	V	2S	85	6.1	680	0.60	410	70	8	25.1	4.8/-	37/-	26.8	208
Boeing 737	V	3S	110	9.1	795	0.75	580	91	8.8	28.4	4.7/1.6	32/11	30	204
Boeing 727C	V	3S	180	9.1	920	0.84	540	150	7.2	32.9	7.7/2.3	61/18	41.5	327
Airbus A300 B2	V	2S	270	9.8	890	0.70	550	260	7.7	44.8	9.4/2.8	66/20	52	364
Douglas DC 10/30	V	3S	330	9.5	880	0.82	796	360	7.5	50.4	10.7/2.7	79/30	52	362
Boeing 747	V	4S	470	10.7	950	0.80	630	511	7.0	50.6	16.6/4.1	113/28	60.2	406
Concorde	OF	4S	144	15.6	2180	2.04	480	358	(1.7)	25.6	27.7/-	308/-	62	465

Key: SF Glider Aircraft M Sports Motor Aircraft
 G Business Travel Aircraft V Commercial Aircraft
 OV Supersonic Commercial Aircraft P Propeller Drive
 S Turbojet Engine

TABLE 2

		AIRBUS A300	Laminar AIRBUS /	AIRBUS Without Profile Resistance
Profile Resistance	c_{WP}	0.0060	<u>0.0020</u>	0
Empennage Resistance	c_{WL}	0.0027	<u>0.0009</u>	0
Fuselage Resistance	c_{WR}	0.0092	0.0092	0.0092
Gondola Resistance	c_{WG}	0.0005	0.0005	0.0005
Other Resistance	c_{Wo}	0.0005	0.0005	0.0005
Noninduced Resistance	c_{WO}	0.0189	0.0131	0.0102

Table 2 Assumed data for a commercial aircraft on the AIRBUS basis. Wing Area $F = 260 \text{ m}^2$, Span $b = 44.8 \text{ m}$, Extension $A = 7.73$, Effective Extension $A_{\text{eff}} = 7.0$, Elevator and Vertical Tail Area Surface $F_L = 114.7 \text{ m}^2$. $c_{WL} = c_{WP} \cdot \frac{F_L}{F}$;
 $c_{WR} = 0.001 \cdot \frac{L}{D}$ (L=Fuselage length, D = Fuselage diameter).

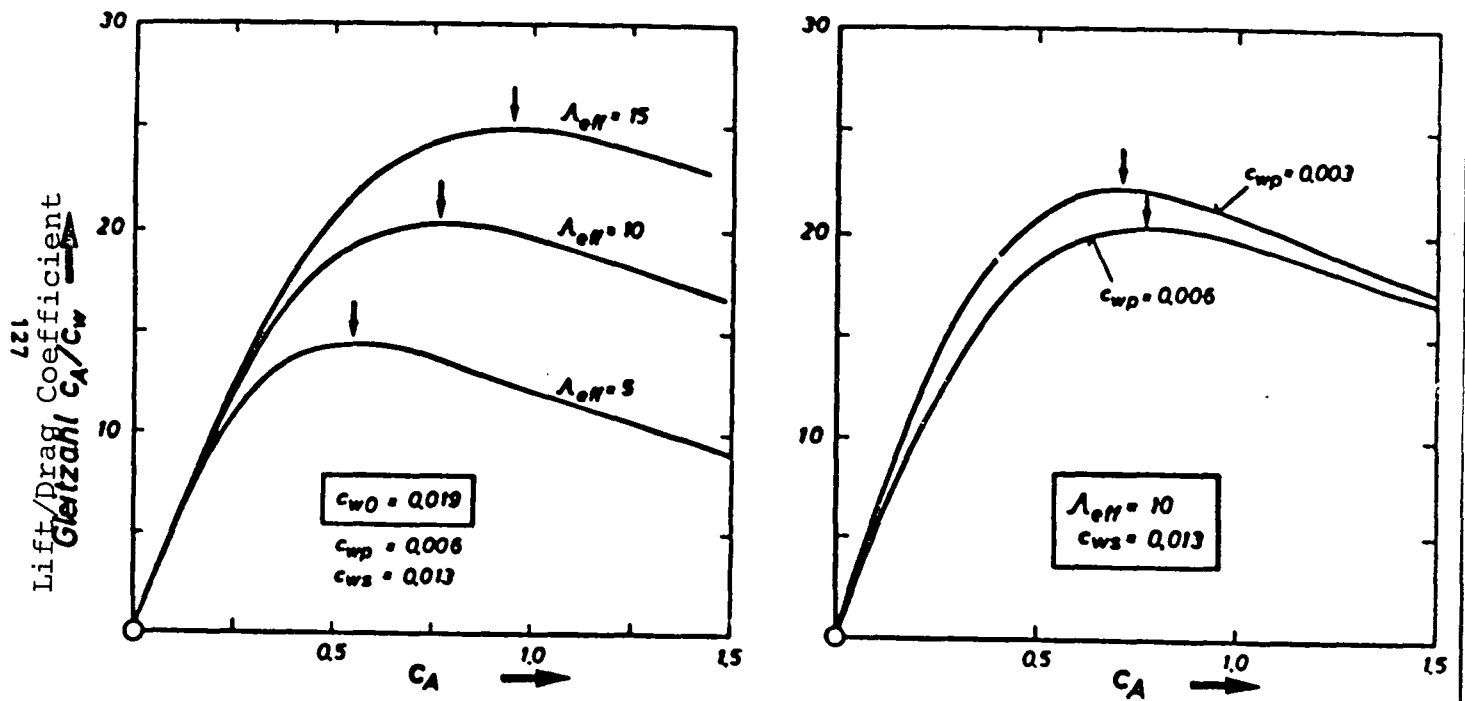


FIGURE 1 Variation of the Lift/Drage Coefficient $E = c_A/c_W$ over the lift coefficient on the

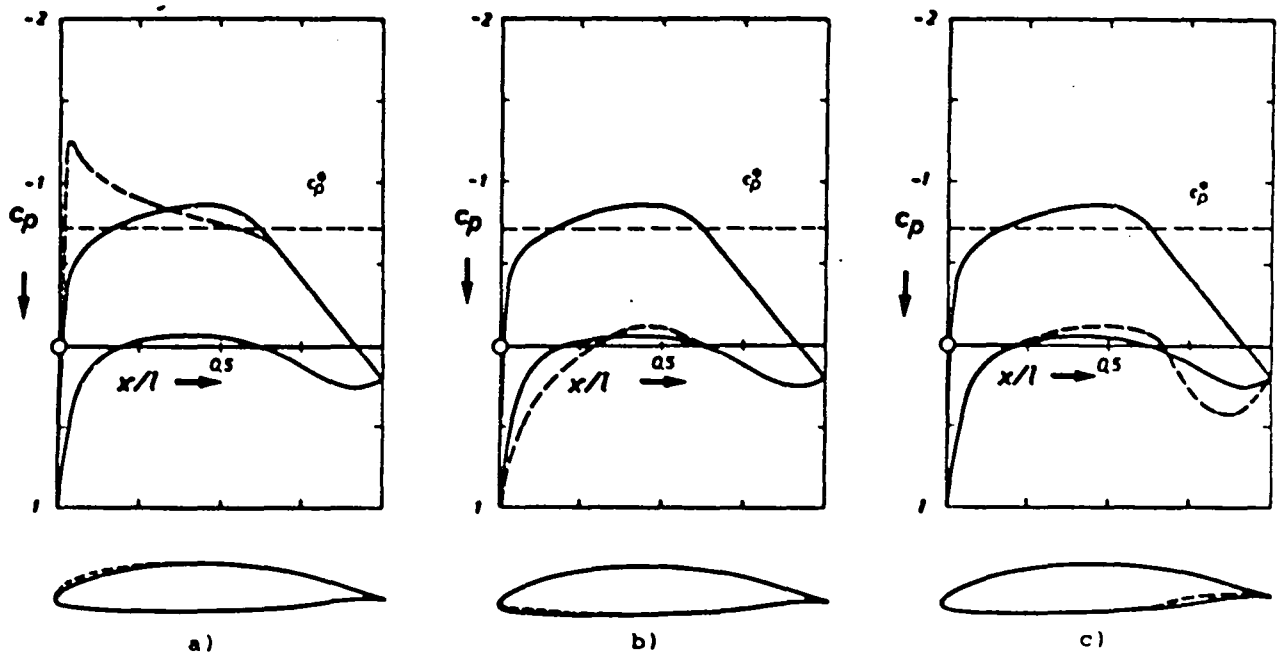


FIGURE 2 Possibilities for increasing the lift on a profile

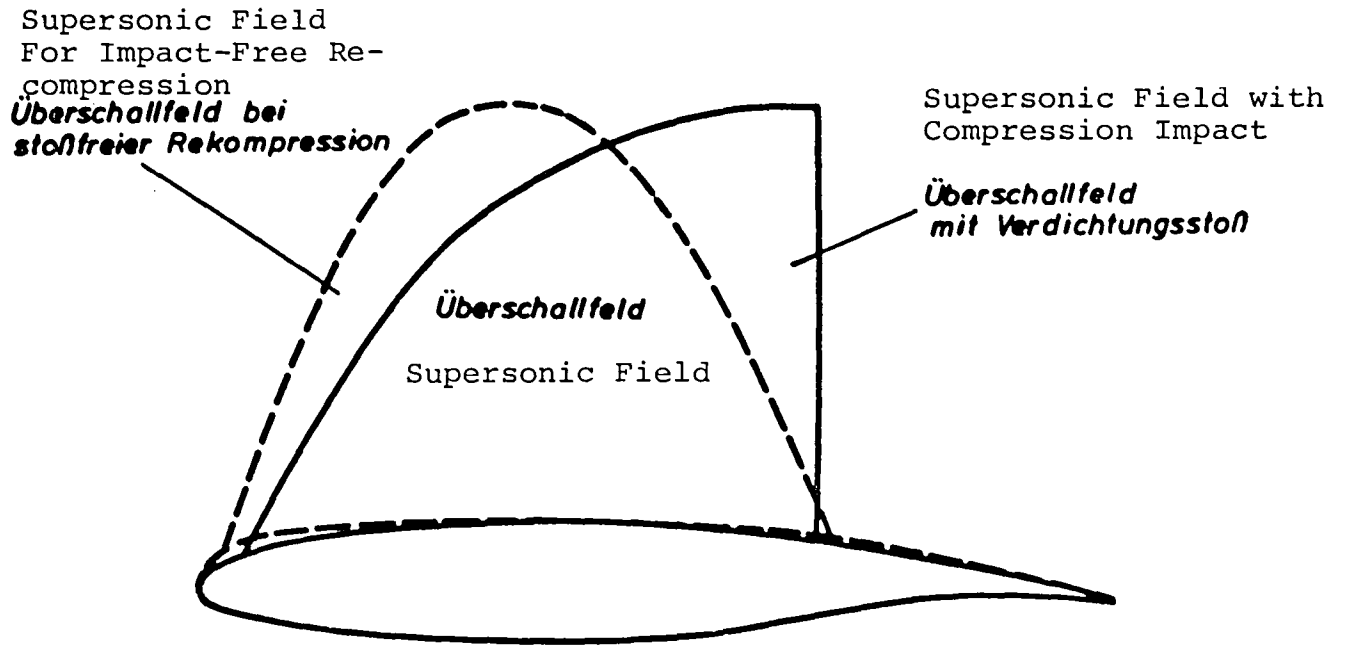


FIGURE 3 Contour and Supersonic Field of Transsonic Profiles with and without Compression Impact

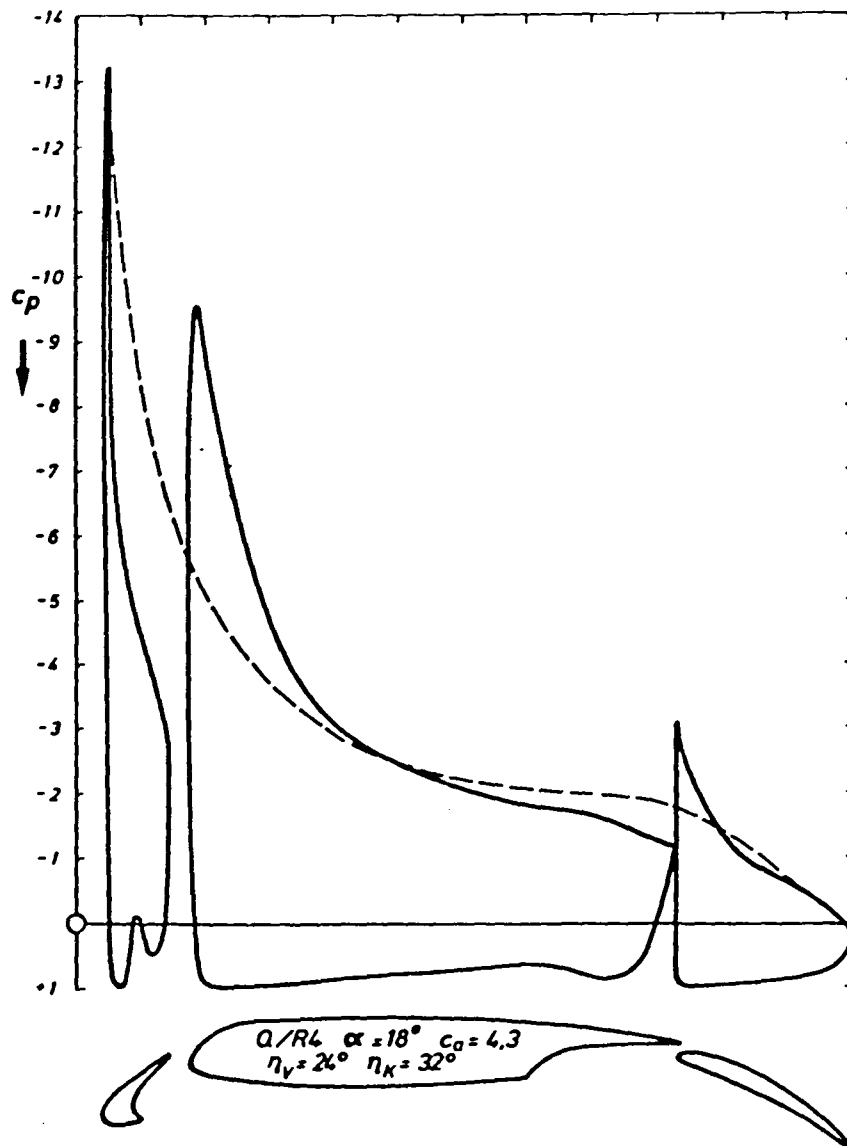


FIGURE 4 Pressure ratios on a high lift system with and without Slits

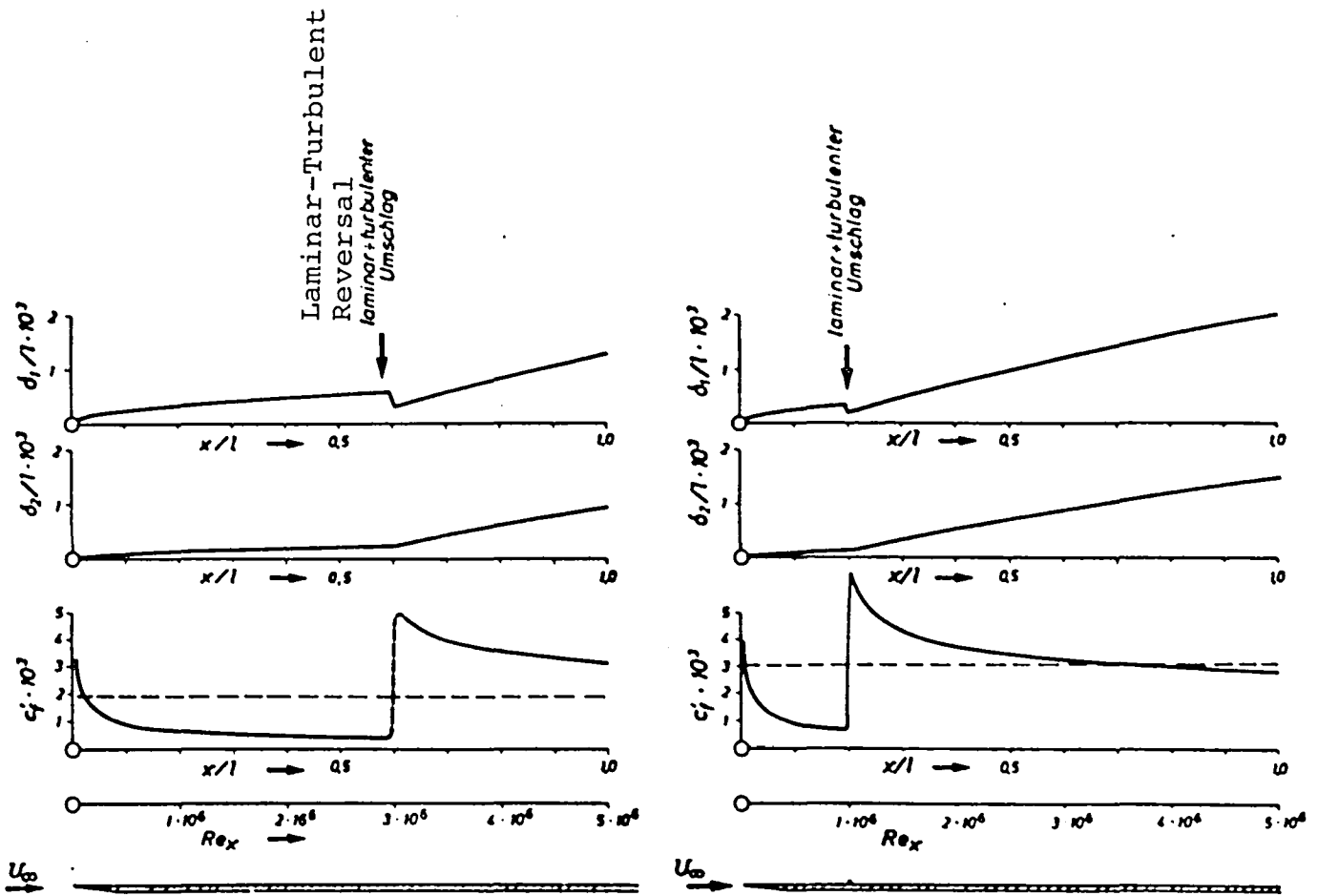


FIGURE 5 Boundary Layer Displacement Thickness δ_1/l , Pulse loss Thickness δ_2/l and Local Resistance Coefficient c_f' of the Plane Plate with Laminar Turbulent Reversal.

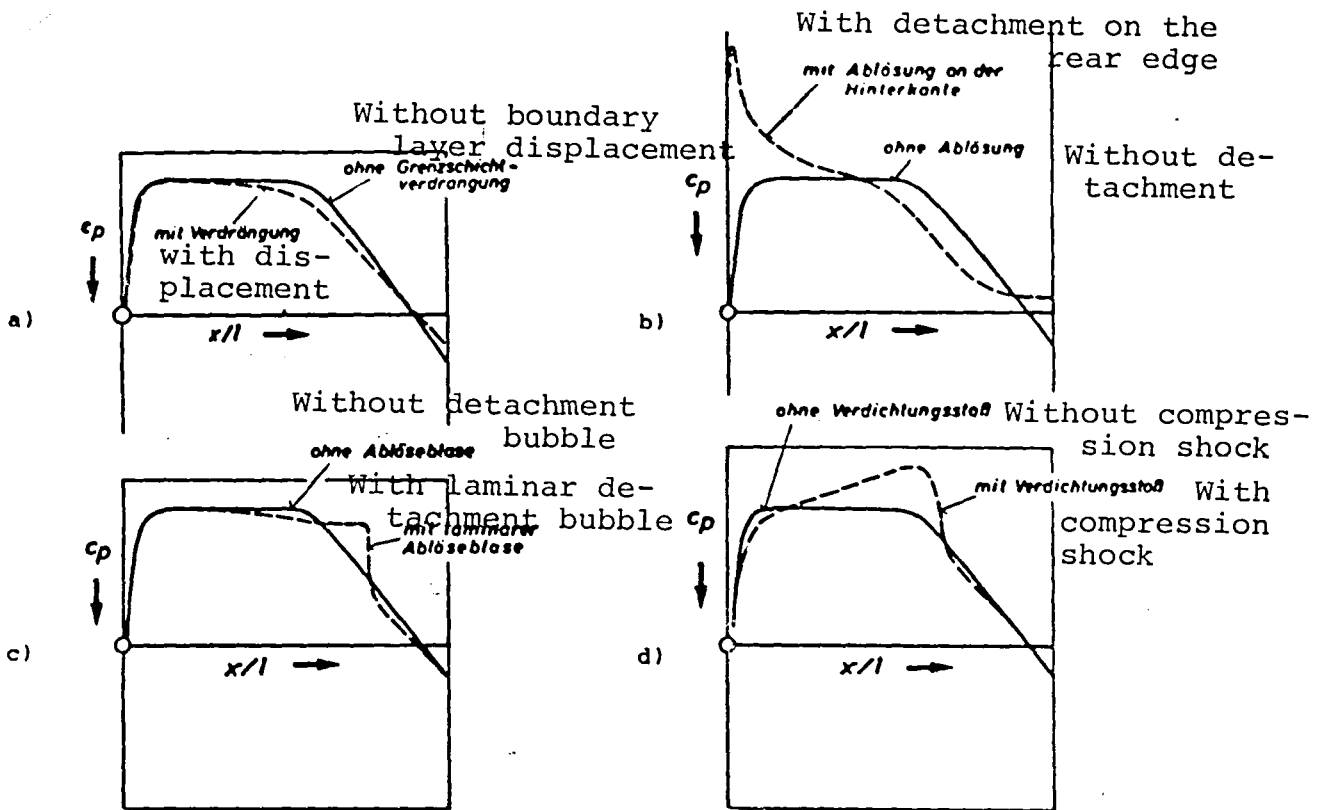
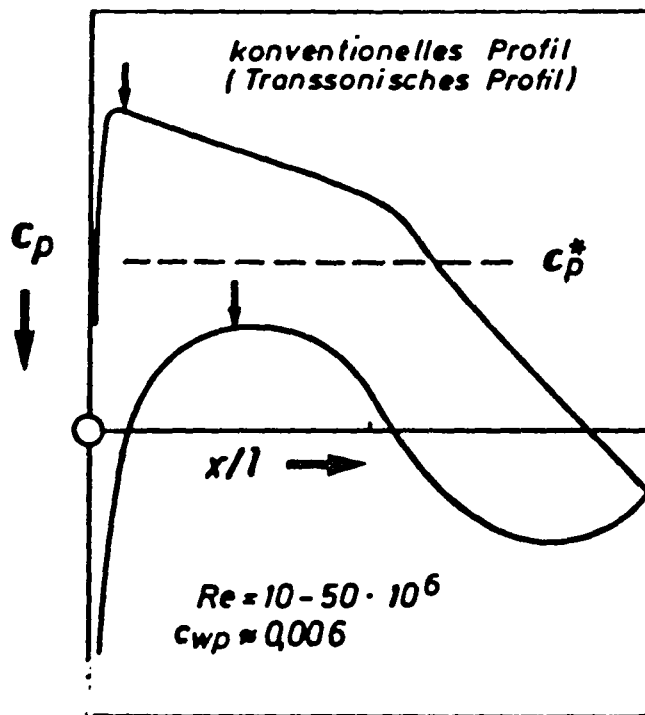


FIGURE 6 Forms of Occurrence of Pressure Resistance on the Top of the Profile



Conventional Profile (Transsonic Profile)

FIGURE 7 Pressure Distribution of a Transsonic Profile of Modern Layout

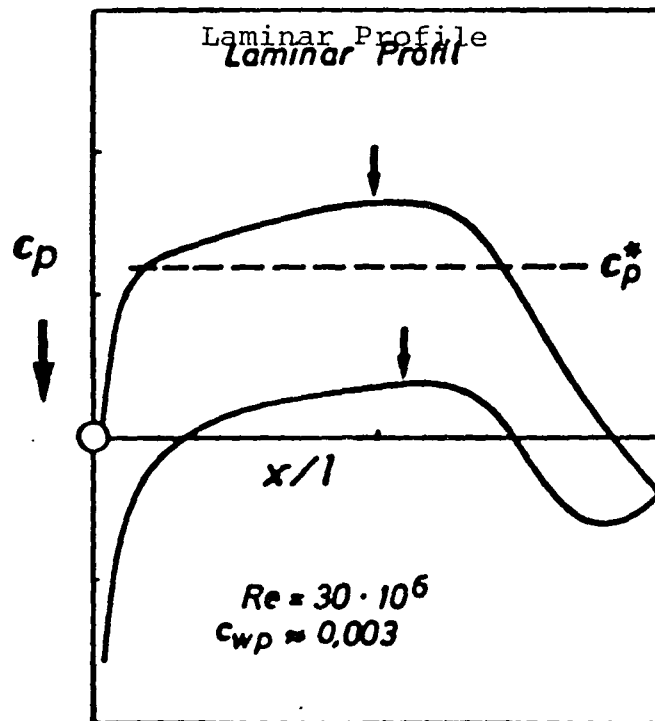


FIGURE 8 Pressure Distribution of a Transsonic Laminar Profile for $Re = 30 \cdot 10^6$ (Commercial Aircraft)

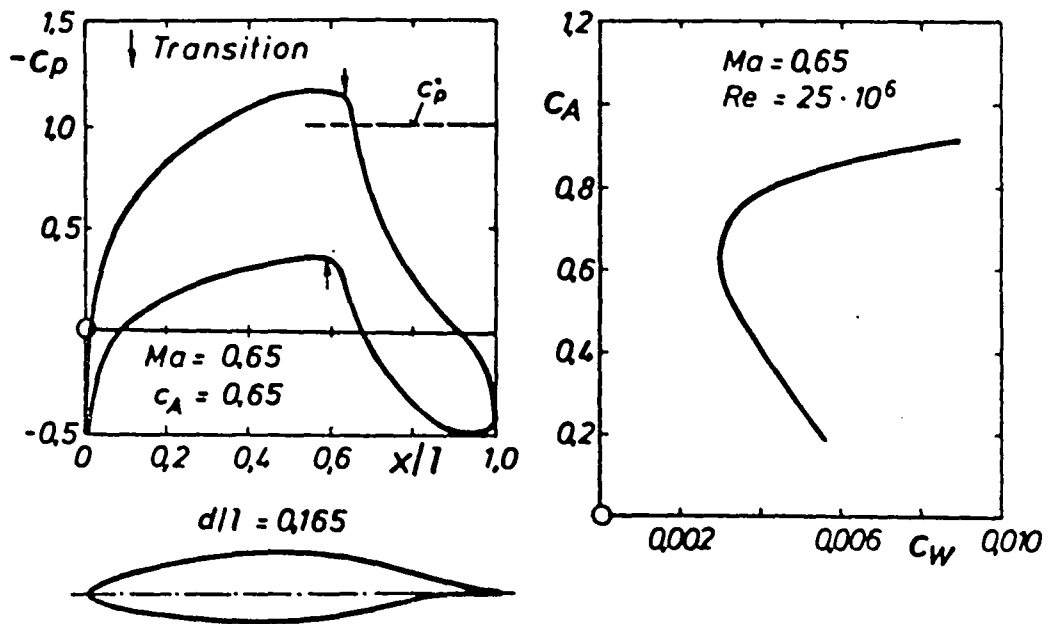


FIGURE 9 Preliminary Design of a Laminar Profile for $Re = 25 \cdot 10^6$ and $Ma = 0.65$ $d/l = 0.165$ Calculated Resistance Polar Curve

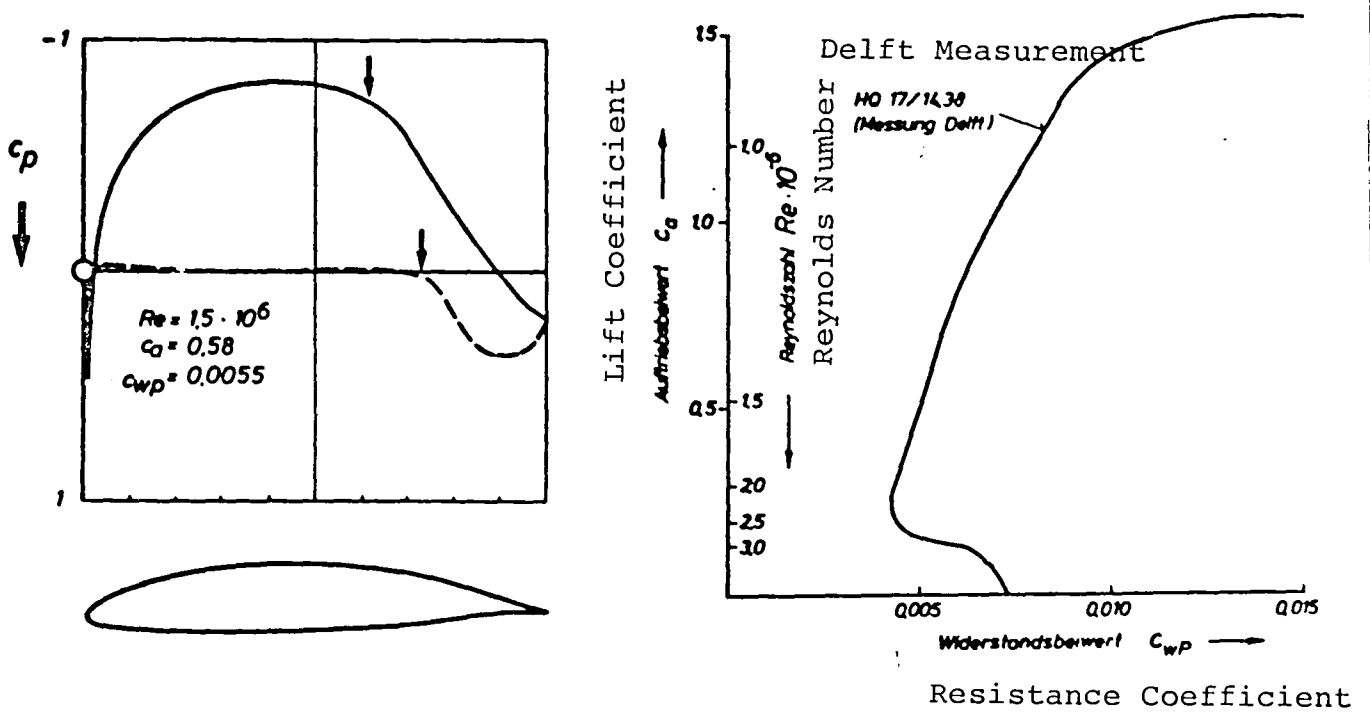


FIGURE 10 Distribution and Envelope of the Resistance Polar Curve of Plain Flap Profile HQ 17/14.38

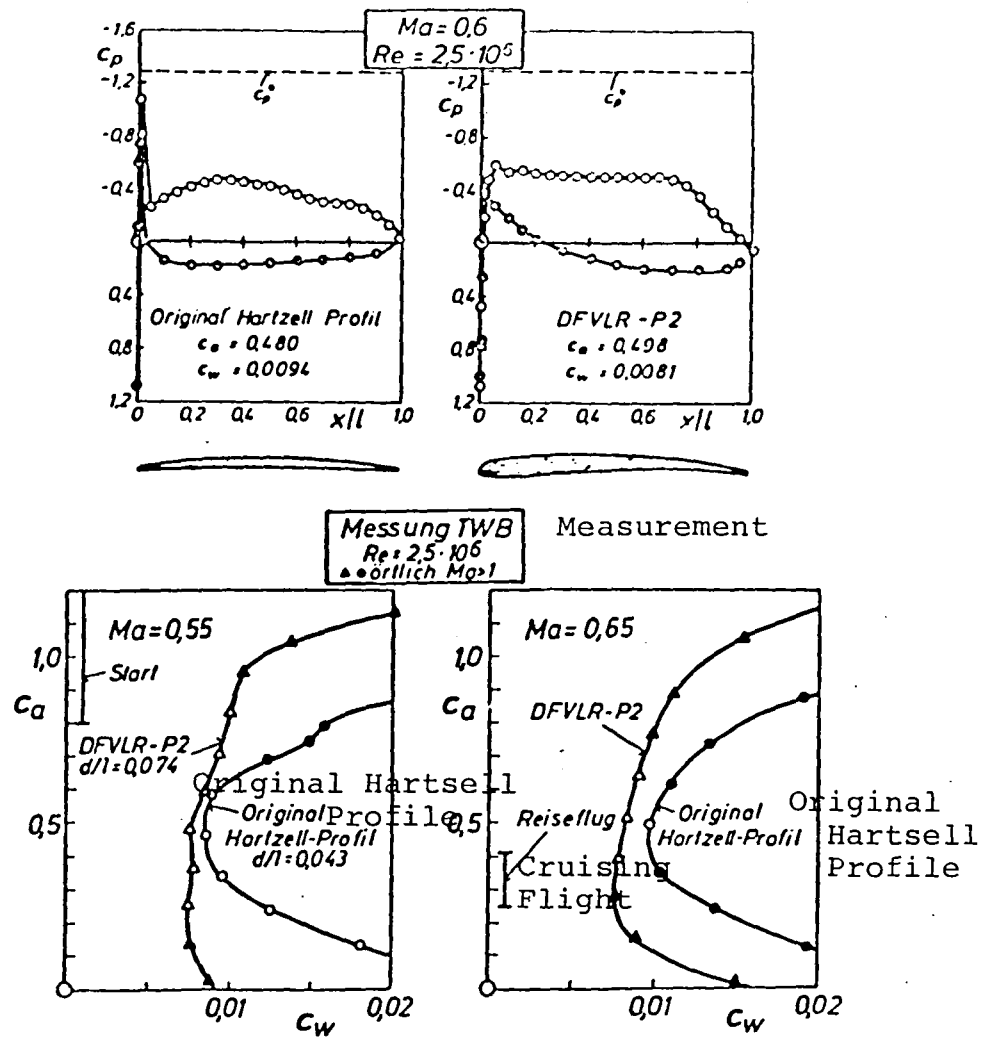


FIGURE 11 Propeller Profile DFVLR-P2 as Compared with a Commercial Propeller Profile

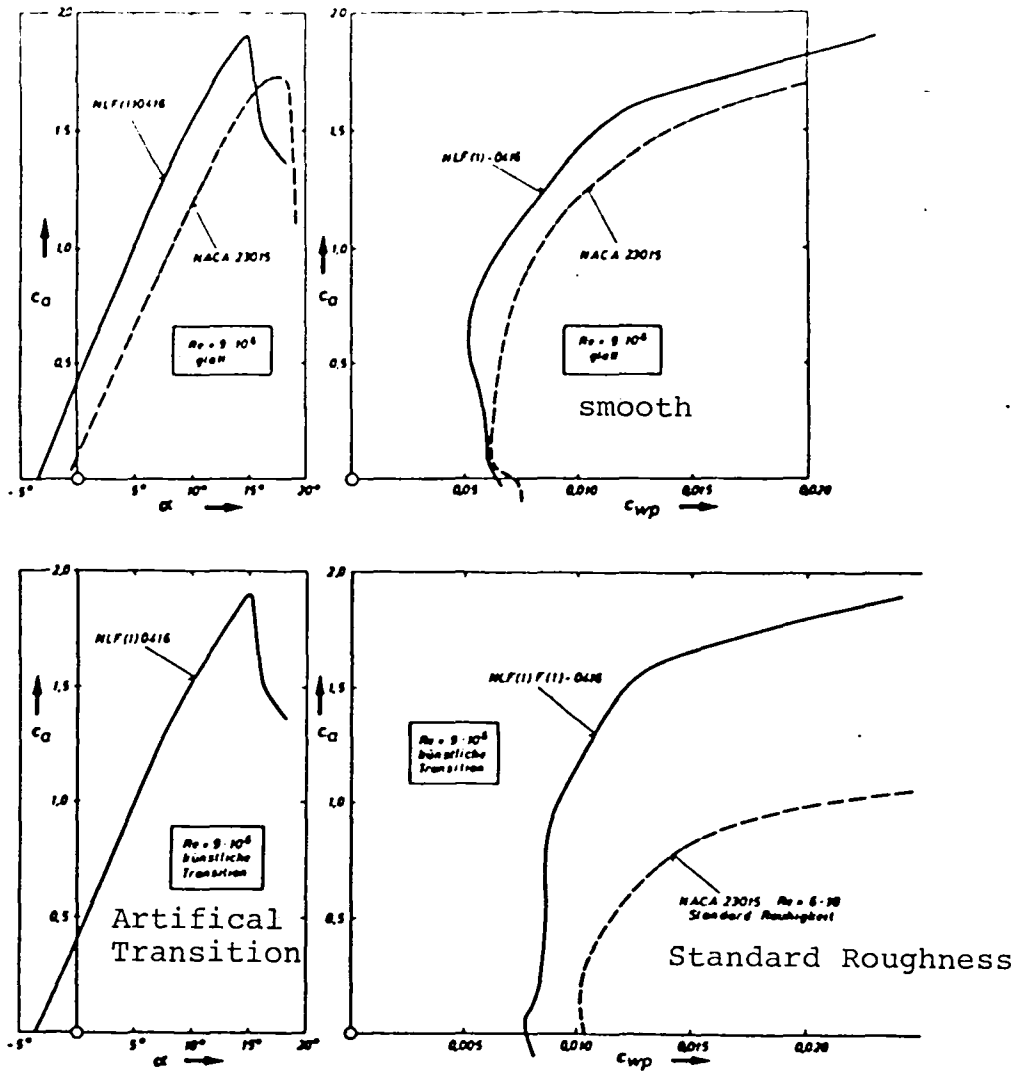


FIGURE 12 Polar Curve of the Laminar Profile NAS NLF (1) 0416 as Compared with the NACA 23015 Profile

LANGLEY RESEARCH CENTER



3 1176 00518 8140